

Force-Displacement Model of Compliant Mechanisms using Assur Sub-Chains

S. Durango* J. Correa† O. Ruiz‡ M. Aristizabal§
CAD CAM CAE Laboratory, EAFIT University
Cr 49 No 7-sur-50, Medellín, Colombia

J. Restrepo-Giraldo¶ S. Achiche||
Engineering Design and Product Development
Technical University of Denmark
Productionstorvet, building 426, 2800 Kgs, Lyngby, Denmark

Abstract— *This article develops a modular procedure to perform force-displacement modeling of planar flexure-based compliant mechanisms (CMs). The procedure is mostly suitable for planar lumped CMs. To achieve the position analysis of CMs requires: (i) to implement the kinematic analysis as for ordinary mechanisms, (ii) to solve equilibrium problem by means of a static analysis and (iii) to model the flexures behavior through a deflection analysis. The novel contribution of this article relies on the fact that a division strategy of the CM into Assur sub-chains is implemented, so that any CM subjected to such disaggregation can be accurately modeled. For this purpose a mathematical model for leaf-spring flexure type is presented and used through this paper. However any other flexure model can be used instead. To support the technique, a three Degrees-Of-Freedom (3-DOF) flexure-based parallel mechanism is used as case study. Results are compared to a Finite Element Analysis (FEA).*

Keywords: Force-displacement model, compliant mechanism, large deflection analysis, Pseudo-Rigid Body Model, Assur group.

I. Introduction

Compliant mechanisms (CMs) concern those mechanisms which gain their mobility from the deflection of flexible elements rather than from kinematic pairs [1].

Flexure-based CMs are instances of CMs in which the flexibility is located in slender regions that supply a rotation between rigid parts. The narrow flexible regions are denoted as *flexure hinges* or simply *flexures*. The relative rotation between two paired rigid links is obtained through the bending of its connecting flexure. In this sense the flexure has the same function as the revolute joint connecting two rigid links.

Some of the main aspects that encompasses the analysis and design of CMs include the force-displacement behavior, topology optimization and fatigue analysis. The displacement analysis of flexure-based CMs cannot be isolated from the deflection analysis of its flexures. The most common methods used for force-displacement model of flexure-

based CMs are the Pseudo-Rigid-Body Modeling (PRBM) and the finite element analysis (FEA). In PRBM the deflection of flexible elements is modeled by rigid-body systems that have equivalent force-displacement characteristics [2] and the force-displacement behavior of the CM is accomplished using classical rigid mechanisms theory. FEA advantages include a wide choice of analysis type (static, dynamic, modal, thermal, etc.) and analysis of geometries with complex shapes [3].

An alternative force-displacement method where an iterative scheme is used to perform non-linear position analysis of planar CMs is presented by Venanzi et al [4]. The technique considers large deflections and allows for different mathematical models for the compliant kinematic pairs, therefore a modular approach is obtained.

The novel contribution of this article is a new force-displacement model procedure that merges the technique proposed in [4] with a divide-and-conquer strategy, in which a number of flexure-based compliant chains (modules) re assembled to yield almost any practical planar CM, leading to an improved modularity. Two basic compliant chain families are conceived for this purpose:

1. Equivalent driving mechanisms.
2. Equivalent Assur groups.

II. Literature Review

The analysis of flexure-based mechanisms can be classified in two main categories.

1. Strategies in which an equivalent rigid-body mechanism is used to perform kinematic and force analysis [1]. In this strategy, the deflection of the flexures are assessed in two ways.

PRBM. In this model the flexures are replaced with rigid bodies connected by kinematic pairs that attempt to assess their force displacement characteristics. For this purpose, springs are added to the model to account for the flexure stiffness. In [5], a flexure-based five-bar mechanism is designed and analyzed through an established kinematic model. No force analysis model is implemented on the formulation. However, validations are carried out by FEA. In [6], a PRBM with a lumped mass-spring model is implemented in the solution of the dynamics of a three Degrees-Of-Freedom (3-DOF) flexure-based parallel mechanism. The kinetostatic model of a 3-RRR compliant micromotion stage

*E-mail: sdurang1@eafit.edu.co

†E-mail: jcorre20@eafit.edu.co

‡E-mail: oruiz@eafit.edu.co

§E-mail: maristi7@eafit.edu.co

¶E-mail: jdrg@man.dtu.dk (corresponding author)

||E-mail: soac@man.dtu.dk

is derived in [7], the model has a closed form solution and different sets of flexure hinge compliant equations are used and compared with the FEA. It should be noted that the aforementioned references ([5], [6], [7]) use particular kinematic and dynamic solutions for their models.

Euler-Bernoulli flexure models. In this technique the deflected shape of the flexures is calculated directly by solving the Euler-Bernoulli equation for long-beam like members. This differential equation can be solved either by using a numerical method [4], [8], e.g. finite differences, or by the implementation of elliptic integrals [9], [10], e.g. solved by numerical integration or series expansion. An input/output model of an XY micromanipulator is presented in [8] in which a full kinematic model that considers the elasticity of the whole CM is proposed allowing to establish the kinematic relationships between output motion and input variables. An iterative technique in which the equivalent rigid-body mechanism dimensions are updated by a large deflection analysis is proposed in [4]. Several types of flexures models can be included into the formulation. The technique can be used to achieve the mechanism pose and required driving loads when subject to a set of input conditions (external load and input links prescribed rotations).

2. Strategies in which FEA are used to solve the force-displacement problem. In [11] a compliant parallel-guiding mechanisms is designed and both, its force-displacement model and guiding accuracy are obtained through FEA. Reference [12] presents a study of the mobility of different types of flexure hinges. A Roberts-Chebyshev straight-line mechanism is analyzed to validate the study. The design of a compliant robotic wrist able to perform spherical motions is discussed in [13]. The inverse and direct kinematics and the design of its flexures are computed by FEA.

Contribution. Compared to the PRBM the procedure proposed in this article represents both a more accurate model and a general approach in which a wide variety of flexure-based CMs can be assessed without the use of closed-form kinematics solutions. Instead, a chain-based analysis technique supported in the Assur groups concept is designed and implemented.

Results reported in this work present a good match when compared to FEA. In addition, the alternative here presented allows the use of analysis and synthesis tools coming from the rigid-body mechanisms theory.

The article is organized as follows: section III summarizes the the force-displacement iterative technique adopted in this work, section IV presents the new algorithm for the force-displacement model of CMs in which kinematics and force analysis are based on a division of the mechanism into Assur groups, in section V the algorithm is tested with a 3-DOF flexure-based mechanism, finally, section VI develops

concluding remarks.

III. Background

The iterative technique to perform the force-displacement analysis of flexure-based CMs introduced in [4] is suitable for modeling those CM that take the form of ordinary mechanisms whose kinematic pairs have been replaced by flexure hinges. Unlike other methods, such as non-linear FEA or PRBM, the flexures are considered as whole parts that undergo large deflections and are not divided into smaller elements, this allows for a modular approach where the large displacement analysis of different kind of flexures is developed so that a great variety of mechanisms with such flexure hinges can be designed and analyzed.

To achieve the position analysis of CMs requires not only to implement the kinematic relations used for ordinary mechanisms but also to include static (equilibrium) and elasticity equations that rule the flexure behavior into the formulation of the model. In order to implement the kinematic equations, conventional revolute pairs must be introduced between one of the extremities of each flexure and its adjacent rigid segment (Fig. 1), therefore allowing at the current point the relative rotation between the flexure and its rigid segment. Once the input variables are established (input rigid links orientations), the kinematic analysis is solved as for ordinary rigid-equivalent mechanism.

After the kinematic analysis solution is reached, the equilibrium problem is solved by means of a static analysis to the rigid-equivalent mechanism on its new configuration. The static analysis returns the internal forces acting in each joint together with the moments to be applied on the input links in order to achieve their prescribed orientations and equilibrate the external loads acting on the mechanism.

Finally, the flexure elastic behavior is modeled by means of a deflection analysis where each flexure present in the CM is modeled as an independent part. A differential equation that allows to model large deflections of the flexure hinge is utilized to relate the deflected shape of each flexure with the load applied upon it, which results in the computation of a new rigid-equivalent mechanism geometry. In this manner new results of kinematic and force analysis are obtained what leads to a loop. The loop is iterated until all variables converge.

IV. Force-Displacement Model of Compliant Mechanisms using Assur Sub-Chains

The methodology of this work relies on the division of the CM into rigid-equivalent sub-chains derived from its kinematic structure, so that kinematic and force analysis can be solved independently (within an iteration step) for the sub-chains instead of formulating a solution for the entire mechanism. After that, a deflection analysis is carried out to each flexure within the mechanism where new equivalent dimensions of the sub-chains are estimated. The procedure is presented in algorithm 1, and stated through this

section in three steps. Prior to that, the topology and geometry of the rigid-equivalent mechanism must be determined together with its disaggregation into driving mechanisms and Assur groups, as pointed out in sections IV-A and IV-B.

A. Structural analysis of rigid-equivalent mechanism

To perform an structural analysis of the CM, a rigid-equivalent mechanism must be determined. This task can be accomplished by replacing each flexure hinge of the CM by a revolute joint. At this point we are only concerned about the topological characteristics of the rigid-equivalent mechanism. Geometrical characteristics will be determined after the disaggregation into Assur groups of the rigid-equivalent mechanism and its generation principle (generation of a mechanism by the successive joining of Assur groups) are established (section IV-B).

Figure 1 presents a 3 DOF flexure-based parallel mechanism (Fig. 1(a)) and its rigid-equivalent mechanism (Fig. 1(b)). If the rigid-equivalent mechanism is simple enough, its disaggregation into Assur groups and the determination of its kinematic structure can be accomplished by inspection. However, if the mechanism possesses a complex kinematic structure, there exist available computational methods that allow the separation of planar mechanisms into Assur groups (e.g. [14]). For the sake of brevity, it is assumed along this work that the disaggregation into Assur groups and the generation principle are established. Two basic groups families are considered:

1. One degree of movability kinematic chains formed by a driving link, a revolute joint and the fixed link and denoted as driving mechanisms.
2. Zero degrees of movability kinematic chains denoted as Assur groups.

The generation principle of a mechanism can vary depending on the selection of its input links. There exist several types of Assur groups which a mechanisms can be formed of. Nevertheless, only CMs whose rigid equivalent mechanism posses Assur groups of the second and the third class within their kinematic structure are to be considered through this article. The combination of this groups yield almost any practical planar mechanism [15]. Figure 2 illustrates the generation principle of a 3-DOF flexure-based parallel mechanism after its three links connected to the ground have been selected as driving links.

B. Convention for rigid-equivalent mechanism determination

The initial step in the iterative force-displacement modeling of CMs is the calculation of its rigid-equivalent mechanism kinematics. Prior to that, it is necessary to determine the geometry of the rigid-equivalent mechanism. The dimensions of the links are determined by the location of the equivalent revolute joints. Moreover, the location of the joints is determined specifically by each Assur group

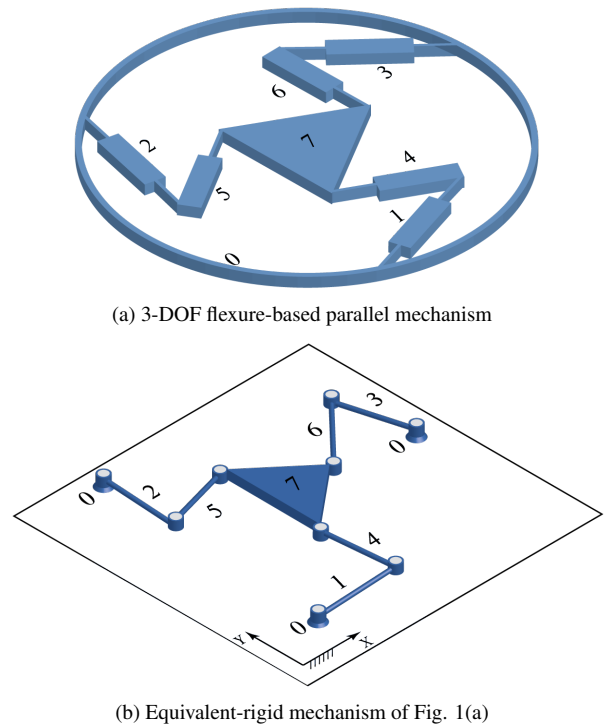


Fig. 1. 3-DOF flexure-based parallel mechanism and its rigid-equivalent mechanism

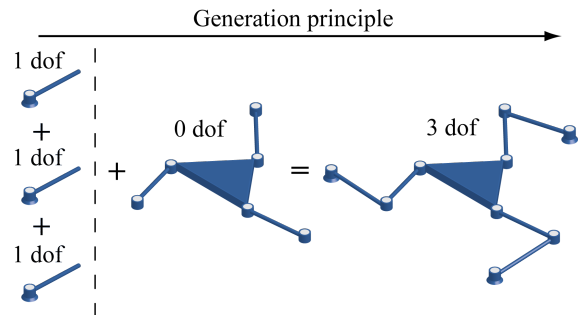


Fig. 2. $3RRR$ mechanism generation principle

type present in the generation principle. Two kind of joints within the Assur groups are considered :

1. *External* or *free* joints: joints that connect the Assur group to other groups, the fixed link or the driving links.
2. *Internal* joint: joints that connect two Assur group internal links.

The following convention to locate the equivalent revolute joints is adopted:

1. Equivalent *external* joint. The revolute joint is located in the edge between the rigid section and the flexure (Fig. 3).
2. Equivalent *internal* joint. The revolute joint is located in any two of the edges between the joined rigid sections and the flexure (Fig. 3).

According to convention (1) and (2), the equivalent second and third class Assur groups are defined as illustrated in Fig.

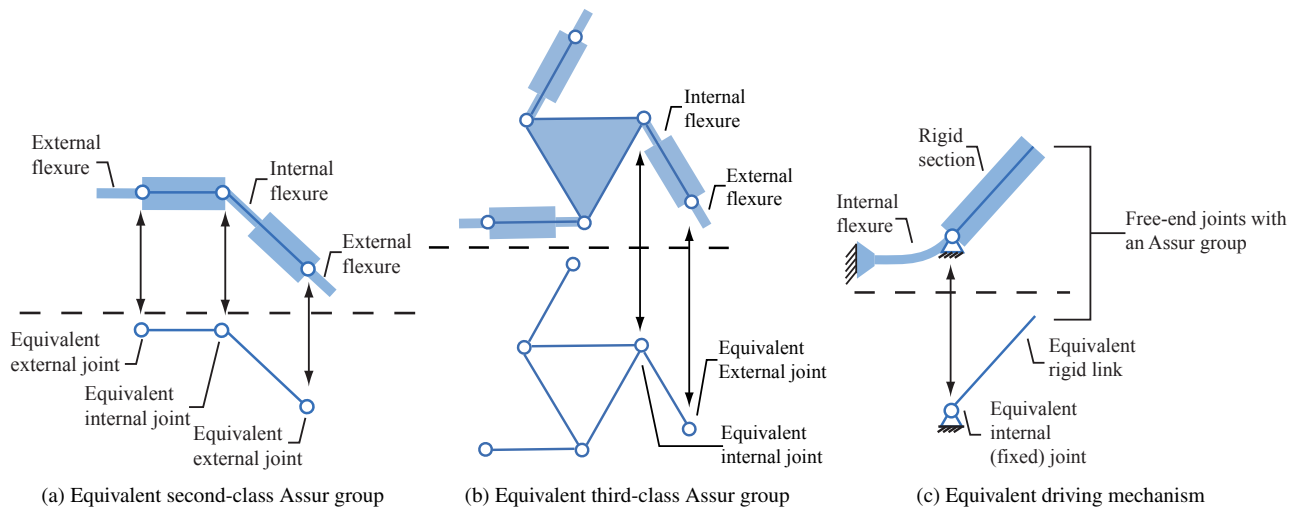


Fig. 4. Equivalent Assur groups and driving mechanism convention

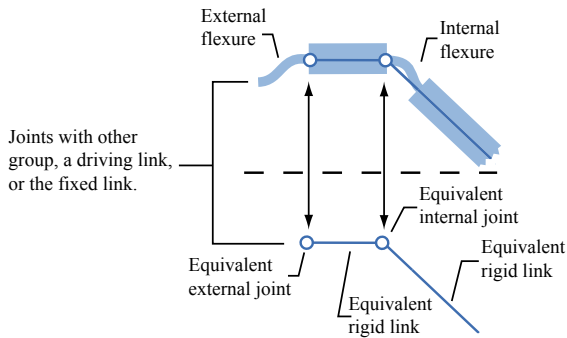


Fig. 3. Equivalent Assur groups convention

4(a) and Fig. 4(b) respectively. Similarly, Fig. 4(c) shows the convention to assign the revolute joint of an equivalent driving mechanism. The purpose of locating the revolute joints between one of the extremities of the flexure and one of its adjacent rigid segments is to ensure that the internal forces acting coming from the static analysis, are located such that each flexure can be modeled as a constant cross-section cantilever beam with its free tip under the action of two forces, F_x and F_y , and a moment M (Fig. 8).

C. Force-displacement model

The concept of modular kinematics and force analysis is based on a divide-and-conquer approach: the analyses are solved by the disaggregation of the mechanism into simpler kinematic chains that can be analyzed in a hierarchical order rather than analyzing the complete mechanism. The kinematic chains are the so called driving mechanisms and Assur groups and the hierarchy is determined by the order in which the chains must be added to form the mechanism (generation principle) [16]. An Assur group is defined as a determined kinematic chain that cannot be disaggregated into lower class Assur groups [15], [16]. As a consequence,

its kinematic and static models can be stated independently being this property the keystone of the modular approach. Standard solutions for the kinematics and statics of different classes of groups are available in the literature [15], [16]. The solution of the modular kinematics and force problems requires:

1. To know the generation principle of the mechanism as pointed out in section IV-A.
2. To have the solution modules of the position and force problems of the driving mechanisms and Assur groups within the generation principle of the mechanism.
3. To have the geometry (dimensions) of the equivalent driving mechanisms and Assur groups within the generation principle of the mechanism as pointed out in section IV-B.

Considering conditions (1-3), the force displacement procedure is carry out in the following manner:

Step 1. Modular kinematics

Given:

1. A rigid-equivalent mechanism reference configuration (non-deflected configuration at fist iteration) determined by:
 - (a) The position of driving mechanisms joints given by the set $\{\mathbf{r}^{D1}, \dots, \mathbf{r}^{D\omega}\}$.
 - (b) The position of Assur groups joints given by the set $\{R^{A1}, \dots, R^{A\Omega}\}$.

Ω and ω are respectively the number of Assur groups and driving mechanisms within the generation principle of the mechanism. \mathbf{r}^{Di} is the position vector of the i th driving mechanism revolute joint and R^{Aj} is the set of position vectors of the j th Assur group revolute joints. Both the \mathbf{r}^{Di} vector and the R^{Aj} set of vectors are referenced to the global coordinate system (OXY).

Algorithm 1 Force-Displacement Model of Compliant Mechanism.

Require: $Mech_relax_config$ rigid equivalent mechanism relaxed configuration,
 $\mathbf{q} = [q_1 \ q_2 \ \dots \ q_\omega]^T$ required orientations of driving mechanisms,
 φ_i flexures geometry and material properties,
 P external loads and application points

Ensure: $Mech_deflect_config$ rigid equivalent mechanism deflected (updated) configuration,
 $\tau = [\tau_1 \ \tau_2 \ \dots \ \tau_\omega]^T$ driving torques to archive the prescribed orientations \mathbf{q} given the external loads P

1: $Mech_ref_config = Mech_relax_config$
2: $M_i = 0$ (* M_i is the i th-flexure internal moment*)
3: $error = tol$
4: **while** $error \geq tol$ **do**
5: (*Step 1. Modular kinematic analysis*)
6: $\{Mech_deflect_config, \Theta_i\} = \mathbf{Modular_kinematics}(Mech_ref_config, \mathbf{q})$ (* Θ_i is the i th-flexure effective rotation*)
7: (*Step 2. Modular static analysis*)
8: $\{F x_i, F y_i, \tau\} = \mathbf{Modular_statics}(Mech_deflect_config, P, M_i)$ (* $F x_i, F y_i$ are the internal forces acting on the i th-revolute joint*)
9: (*Step 3. large deflection analysis*)
10: $\{Mech_ref_config, M_i\} = \mathbf{Large_deflection}(F x_i, F y_i, \varphi_i, \Theta_i)$
11: $error = |Mech_deflect_config - Mech_ref_config|$
12: **end while**

2. The prescribed orientation of the driving mechanisms,

$$\mathbf{q} = [q_1 \ q_2 \ \dots \ q_\omega]^T, \quad (1)$$

where \mathbf{q} is a column vector of input joint angles.

Goal. To find:

1. An updated (deflected) rigid-equivalent mechanism configuration determined by:
 - (a) The position of driving mechanisms joints ($\{\mathbf{r}^{D1}, \dots, \mathbf{r}^{D\omega}\}$).
 - (b) The updated position of Assur groups joints ($\{R^{A1}, \dots, R^{A\Omega}\}$).
2. The flexures effective rotation ($\Theta_i, i = 1, 2, \dots, \gamma$, where γ is the number of flexures). Θ_i is evaluated after the position \mathbf{r}^i of every equivalent joint (updated rigid-equivalent mechanism configuration) is determined. If the flexure is placed between two rigid segments whose orientations are described by the α and β angles (see Fig. 5), then the flexure effective rotation referenced to the local coordinate system oxy is given by

$$\Theta_i = \beta - \beta_0 - \alpha + \alpha_0, \quad (2)$$

Eq. (2) reduces to Eq. (3) using the angles differences.

$$\Theta_i = \Delta\beta - \Delta\alpha. \quad (3)$$

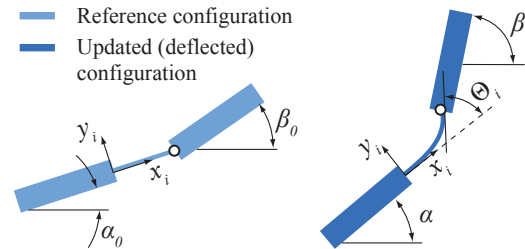


Fig. 5. Flexure effective rotation

The modular kinematic analysis is carry out as illustrated on Fig 6. The mechanism reference configuration is used to calculate the current dimensions of the rigid equivalent mechanism. After that, the position of each revolute joint within the equivalent mechanism is obtained according to the mechanism generation principle. This implies that the driving mechanisms position problem is first solved, what determines the position of any point laying on the driving links that might connect to the remaining Assur groups. As a result, the position (constraints) of the free-joints of the first Assur group in the sequence are obtained.

The solution of the first Assur group position problem provides the free-joint positions of following Assur groups. The sequence advances in the direction of the generation principle until the position problem of all Assur groups are solved.

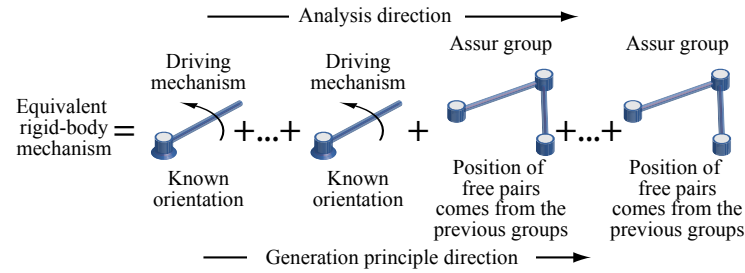


Fig. 6. Kinematic analysis of a rigid-body mechanism

Step 2. Modular force analysis

Given:

1. The rigid-equivalent mechanism updated (deflected) configuration determined by:
 - (a) The position of driving mechanisms revolute joints at updated configuration configuration $(\{\mathbf{r}^{D1}, \dots, \mathbf{r}^{D\omega}\})$.
 - (b) The position of Assur groups revolute joints at updated configuration $(\{R^{A1}, \dots, R^{A\Omega}\})$.
2. The set of external loads (P) applied to the Assur groups and their application points.
3. The internal moment M_i (zero at first iteration) that equilibrates the loads F_{X_i}, F_{Y_i} at the deflected configuration.

Goal. To find:

1. The internal forces (F_{X_i}, F_{Y_i}) acting on each joint of the rigid-equivalent mechanism referenced to the world coordinate system OXY .
2. The set of driving loads (τ) that has to be applied to the driving links to equilibrate the external loads (P) and achieve the prescribed rotations (\mathbf{q}).

$$\tau = [\tau_1 \quad \tau_2 \quad \dots \quad \tau_\omega]^T, \quad (4)$$

where τ is a vector of driving loads.

The procedure for the modular static analysis is illustrated on Fig. 7. The solution is achieved sequentially in the opposite direction of the generation principle. First the last Assur group static-problem is solved determining a set of joint reactions that are introduced as external loads acting on the previous groups. After that, the previous group is solved and the sequence goes on until all the groups within the mechanism are solved. Finally, the solution of each driving mechanism equilibrium-problem is reached determining the driving loads (τ) and the fixed joint reactions.

Step 3. Large deflection analysis

After kinematic and force analysis problems are solved, the next step is to model the behavior of the flexure hinges through a deflection analysis stated in the following manner:

Given:

1. The flexures effective rotation (Θ_i).

2. The internal forces (F_{X_i}, F_{Y_i}) acting on each revolute joint (flexure hinge free-end) of the rigid-equivalent mechanism.
3. The flexure geometry and material properties (φ_i).

Goal. To find:

1. The flexures free-end position vector (\mathbf{r}_i) at deflected configuration. This corresponds to the correction to the position correction of all joints and therefore, to the new mechanism reference configuration required for the next iteration.
2. The internal moment M_i that equilibrates the loads F_{X_i}, F_{Y_i} at the deflected configuration.

The deflected shape of a flexure is described by its relative free-end position vector (${}^{oxy}\mathbf{r}_i = \bar{\mathbf{u}}_i + \bar{\mathbf{v}}_i$) and its free-end rotation (Θ_i) (Fig. 8). The left superscript oxy refers \mathbf{r}_i to the flexure local coordinate system.

Similarly, the load applied to the flexure is described by the forces (F_{x_i}, F_{y_i}) and the moment M_i acting on the flexure hinge free-end (Fig. 8). It should be noted that the forces (F_{x_i}, F_{y_i}) are the axial and shear components of the force acting on the flexure hinge and they correspond to the projection of the global forces (F_{X_i}, F_{Y_i}) to local coordinate system oxy .

The following deflection analysis is adopted from the work by S.Venanzi et al. [4], and its summarized as follows:

The Euler-Bernoulli equation (for long-beam like members) is used to model each flexure hinge when large deflections are considered by relating both the deflected shape and the forces applied upon it. The non-linear aspect is introduced by combining the bending effects of three end loads (F_{x_i}, F_{y_i}, M_i) , as it is well know that linear displacement theory disregards the contribution of the axial force to the bending.

The bending moment acting on a section s is defined as:

$$M(s) = M + Fy(u - x(s)) - Fx(v - y(s)), \quad (5)$$

where s is a linear coordinate along the beam, $(x(s), y(s))$ are the local coordinates of the point (s) where the bending moment is evaluated and (u, v) are the local coordinates of the free-end (Fig. 8). The Euler-Bernoulli differential equation states

$$\frac{d\theta(s)}{ds} = \frac{M(s)}{EI}, \quad (6)$$

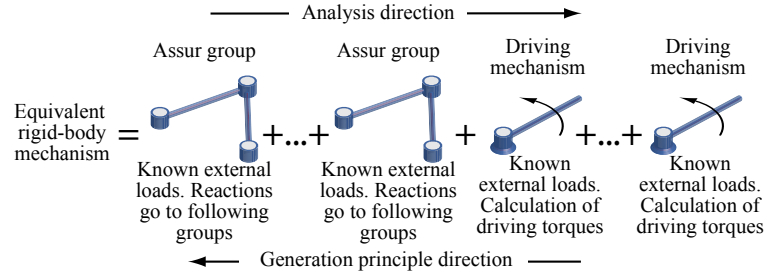


Fig. 7. Static analysis of a rigid-body mechanism

where $\theta(s)$ is the beam rotation, E is the material elastic modulus and I the cross section area moment of inertia. The following identities are valid for a point of the deflected beam:

$$\begin{aligned} \frac{dx(s)}{ds} &= \cos \theta(s), \\ \frac{dy(s)}{ds} &= \sin \theta(s). \end{aligned} \quad (7)$$

Combining and reorganizing Eqs. (5) – (7), the Euler – Bernoulli equation for a deflected beam is formulated as a system of first order differential equations (Eq. (8)).

$$\frac{d}{ds} \begin{bmatrix} \theta(s) \\ x(s) \\ y(s) \end{bmatrix} = \begin{bmatrix} \frac{M + Fy(u-x(s)) - Fx(v-Y(s))}{EI} \\ \cos \theta(s) \\ \sin \theta(s) \end{bmatrix}, \quad (8)$$

subject to the boundary conditions

$$\begin{bmatrix} \theta \\ x \\ y \end{bmatrix} \Big|_{s=0} = \begin{bmatrix} 0 \\ 0 \\ 0 \end{bmatrix}, \quad \begin{bmatrix} \theta \\ x \\ y \end{bmatrix} \Big|_{s=L} = \begin{bmatrix} \Theta \\ u \\ v \end{bmatrix}. \quad (9)$$

The boundary conditions are applied to both bounds of the independent variable s , which varies between 0 and L for the length of the beam. Six parameters are related in Eq. (8) and (9): M , the moment on the beam free end, F_x and F_y , the components of the load acting on the free-end of the beam (referenced to the local coordinate system oxy), the effective rotation Θ , and the components of the relative free-end position vector of the beam (u, v) .

It should be noted that the flexure free-end position vector \mathbf{r}_i (see Sec.IV, step 3, goal 1) corresponds to the projection of the relative free-end position vector ${}^{oxy}\mathbf{r}_i$ to the global coordinate system (OXY)

If the effects of the internal axial force acting on the beam are added to Eq. (8), then the accuracy of the solution is reported to be increased [4]. The boundary value problem solution required the parameters Θ , F_x and F_y as known inputs and provides the output parameters M , u and v . A numerical method might be implemented for this purpose ([4], [8]).

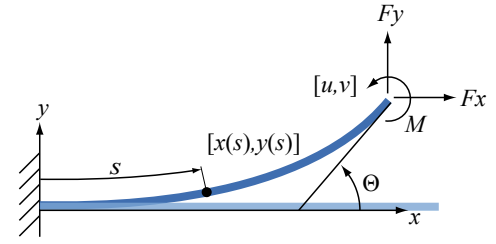


Fig. 8. Flexure hinge deflection analysis [4]

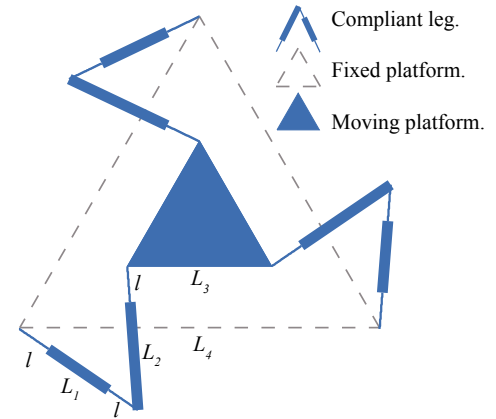


Fig. 9. Compliant mechanism case study

V. Results

In this section the force-displacement model of a 3-DOF planar CM is performed. The symmetrical mechanism is capable of set its end-effector pose and consists of an equilateral moving platform connected by three identical compliant legs to an equilateral fixed base (Fig. 9). Each compliant leg is formed by an alternating pattern of three flexures connect two rigid segments. The mechanism is actuated from the rigid elements connected to the base. Dimensions are described on Table I, and aluminum 7075 ($E = 70$ GPa) is assumed as material.

A. Generation principle

After the flexures are replaced with revolute joints, the topology of the rigid equivalent mechanism is obtained (Fig. 1). If the three links connected to the fixed base are

Parameter	Value
l	10 mm
L_1	20 mm
L_2	30 mm
L_3	40 mm
L_4	100 mm
Flexure width	5 mm
Flexure thickness	0.1 mm

TABLE I. Case study dimensions

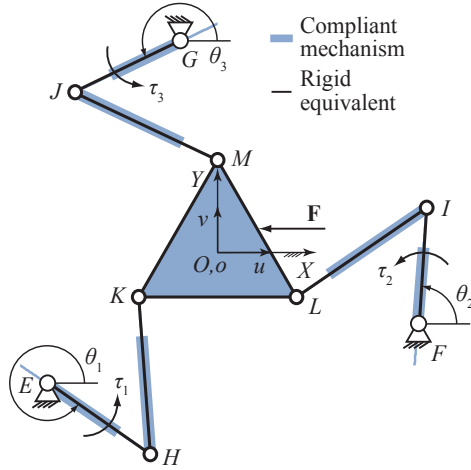


Fig. 10. Compliant mechanism and rigid equivalent

selected as driving links, then the mechanism generation principle is (see Fig. 2):

$$I_R \rightarrow I_R \rightarrow I_R \rightarrow III_{RR-RR-RR}, \quad (10)$$

where I_R denotes a first-class driving mechanism and $III_{RR-RR-RR}$ denotes a third class Assur group.

B. Rigid-equivalent mechanism

Figure 10 shows the assigned rigid-equivalent mechanism at its relaxed position. According to the proposed convention of section IV-B, the mechanism parameters at relaxed configuration are $\overline{EH} = \overline{FI} = \overline{GJ} = 30.00$ mm, $\overline{HK} = \overline{IL} = \overline{JM} = 40.00$ mm, $\overline{KL} = \overline{LM} = \overline{MK} = 40.00$ mm, $\mathbf{r}_E = (-41.74, -34.51)$ mm, $\mathbf{r}_F = (50.76, -18.90)$ mm, $\mathbf{r}_G = (-9.01, 53.40)$ mm, $\theta_1 = -0.599$ rad, $\theta_2 = 1.495$ rad, and $\theta_3 = -2.694$ rad.

C. Force-displacement model

At this point, the previous conditions (see conditions 1–3 of Section IV) to the force-displacement procedure are met.

1. The generation principle of the mechanism is known, expression 10.
2. The solution of the position and force problems of the driving mechanisms and the third-class Assur group are known, e.g. it is possible to solve the position problem

of the third-class Assur group using a numerical strategy such as virtual variable searching. [16].

3. The parameters of the equivalent mechanism at relaxed configuration (see section V-B).

The force-displacement model procedure (section IV), is carry out as follows:

Step 1. Modular kinematics

Given:

1. The rigid equivalent mechanism non-deflected configuration:
 - (a) Position of driving mechanisms revolute joints:

$$\begin{aligned} \mathbf{r}^{D1} &= \mathbf{r}_E, \\ \mathbf{r}^{D2} &= \mathbf{r}_F, \\ \mathbf{r}^{D3} &= \mathbf{r}_G. \end{aligned} \quad (11)$$

- (b) Position of third-class Assur group revolute joints:

$$R^{A1} = \{\mathbf{r}_H, \mathbf{r}_I, \dots, \mathbf{r}_M\}. \quad (12)$$

2. The prescribed orientation of the driving mechanisms:

$$\mathbf{q} = [\theta_1 \ \theta_2 \ \theta_3]^T. \quad (13)$$

Let the following orientations be imposed to input links, $\theta_1 = -0.349$ rad, $\theta_2 = 1.745$ rad and $\theta_3 = -2.444$ rad.

Goal.

The mechanism updated configuration is calculated using the kinematic solutions of the first class driving mechanism and third-class Assur group. For the sake of brevity the H and I joints are proposed as control points through the whole procedure:

1. Third-class group joints positions, R^{A1} :

$$\begin{aligned} \mathbf{r}_H &= (-13.56, -44.78) \text{ mm}, \\ \mathbf{r}_I &= (45.56, 10.65) \text{ mm}. \end{aligned} \quad (14)$$

2. Flexure effective rotations Θ (Eq. (3))

$$\begin{aligned} \Theta_H &= -0.104 \text{ rad}, \\ \Theta_I &= -0.104 \text{ rad}. \end{aligned} \quad (15)$$

Step 2. Modular force analysis

Given:

1. The rigid-equivalent mechanism updated configuration ($\{\mathbf{r}^{D1}, \mathbf{r}^{D2}, \mathbf{r}^{D3}, R^{A1}\}$), calculated in Step 1.
2. The set P of external loads and their application points.

$$P = \{\mathbf{F}, \mathbf{r}_P\}, \quad (16)$$

where $\mathbf{F} = (-400, 0)$ mN and \mathbf{r}_P is the middle point between M and L (Fig. 10).

Goal.

The force analysis is solved using the kinetostatic modules of the third-class Assur group and first-class driving mechanism in two aspects:

1. The joint forces acting on the rigid equivalent mechanism.

$$\begin{aligned}\mathbf{F}_H &= (9.27, -41.06) \text{ mN}, \\ \mathbf{F}_I &= (131.7, 121.6) \text{ mN}.\end{aligned}\quad (17)$$

2. The set of driving loads τ required to equilibrate the mechanism in the prescribed configuration:

$$\tau = [\tau_1 \ \tau_2 \ \tau_3]^T, \quad (18)$$

where $\tau_1 = -0.594 \text{ N mm}$, $\tau_2 = -3.485 \text{ N mm}$, $\tau_3 = 6.107 \text{ N mm}$.

Step 3. Large deflection analysis

Given:

1. The flexure effective rotations ($\{\Theta_E, \dots, \Theta_M\}$), calculated in Step 1.
2. The joint forces ($\{\mathbf{F}_E, \dots, \mathbf{F}_M\}$), calculated in Step 2.
3. The flexures geometry and material properties (Table I).

Goal.

The large deflection analysis is calculated solving the differential equation (8), by means of a standard numerical finite differences algorithm. The solution consists of two aspects:

1. The flexures free-end position vectors ($\{\mathbf{r}_E, \dots, \mathbf{r}_M\}$), used to update the mechanism reference configuration required in Step 1. The updated position of the fixed points H and I are selected as control points:

$$\begin{aligned}\mathbf{r}_H &= (-13.05, -44.00) \text{ mm}, \\ \mathbf{r}_I &= (43.98, 10.62) \text{ mm},\end{aligned}\quad (19)$$

2. The internal moments ($\{M_E, \dots, M_M\}$), used to update the force analysis (see Step 2). The M_H and M_I flexure moments are selected as control points:

$$\begin{aligned}M_H &= 0.468 \text{ N mm}, \\ M_I &= 1.639 \text{ N mm}.\end{aligned}\quad (20)$$

Finally the procedure returns to Step 1 (kinematic analysis), where new dimensions of the rigid-equivalent mechanism are calculated from the mechanism new reference configuration. Steps (1 – 3) are iterated allowing for a maximal difference of $1 \cdot 10^{-6} \text{ N mm}$ between two successive calculations of driving input moments τ . The problem converges after 20 iterations to the following results:

$$\begin{aligned}\tau &= [2.207 \quad -2.286 \quad 9.575]^T \text{ N mm}, \\ \mathbf{r}_o &= (-1.044, -0.062) \text{ mm}, \\ \psi &= -0.277 \text{ rad},\end{aligned}\quad (21)$$

where \mathbf{r}_o and ψ are the moving-platform center position and orientation respectively. The deflected shape of the mechanism is illustrated in Fig. 11.

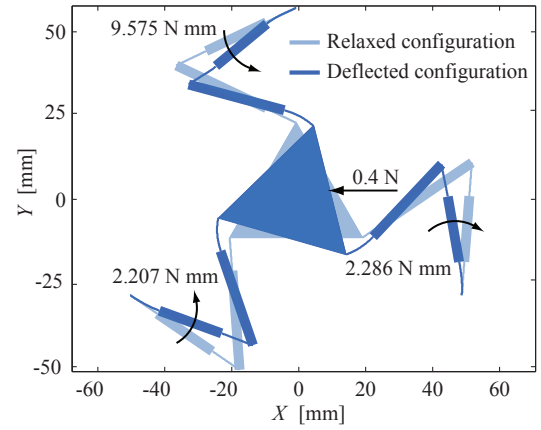


Fig. 11. Compliant mechanism at deflected configuration

D. Workspace analysis and numerical validation

A workspace analysis and numerical validation are performed using the following criteria:

1. No external load is applied to the mechanism.
2. The maximum axial stress at a deflected configuration is limited to 250 MPa.
3. The prescribed rotation range for each driving link is the same and any combination $\mathbf{q} = [\theta_1 \ \theta_2 \ \theta_3]^T$. within that range is evaluated.
4. A numerical validation is performed comparing the force-displacement workspace predictions with nonlinear FEA. For this purpose a large deflection beam element is implemented in ANSYS®.

Figures 12 to 13 illustrate the maximal axial bending stress (Fig. 12) and the end-effector position and orientation errors compared to FEA (Fig. 13 and Fig. 14) in terms of the feasible active-joints workspace (left side of each figure) and its correspondent end-effector workspace (right side of each figure).

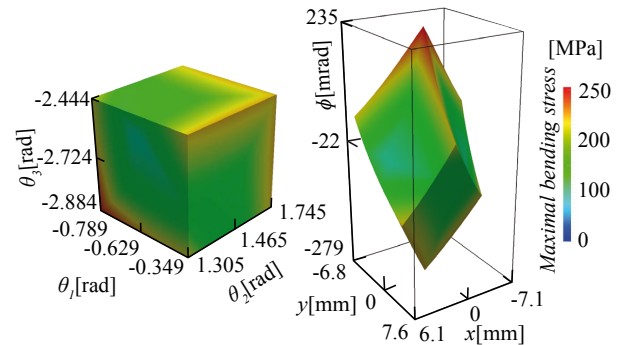


Fig. 12. Joint and end-effector workspaces with maximal axial bending stress (colormap)

VI. Conclusion

This article addresses the force-displacement model of flexure-based planar CMs considering large deflections un-

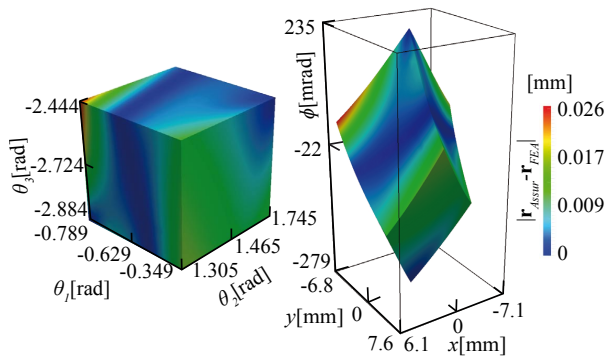


Fig. 13. Joint and end-effector workspaces with End-effector absolute position error compared to FEA (colormap)

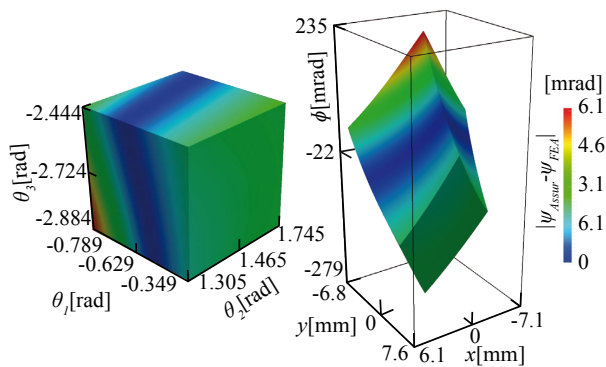


Fig. 14. Joint and end-effector workspaces with end-effector absolute orientation error compared to FEA (colormap)

der quasi-static conditions. A new force-displacement model procedure consisting of three iterative steps, kinematic – force – large deflection analysis, is developed in section IV.

Unlike other procedures, the kinematic and force analysis are solved through the decomposition of a rigid-equivalent mechanism into Assur groups. Such a decomposition and the equivalent joints location are determined using the structural analysis routine and a proposed convention presented in sections IV-A and IV-B. This enables for an extended analysis capability in which the force-displacement model of a wide variety of mechanisms can be assessed depending on the amount of Assur groups available in a kinematic and force analysis solutions library.

To validate the performance of the proposed procedure a 3-DOF CM case study was carried out (section V). Two experiments were conducted. First, the mechanism pose was assessed under an applied load and prescribed orientation of the driving links. And second, a workspace analysis subjected to axial bending stress restrictions. Comparisons with FEA led to a good match, as the maximal error values of the end-effector position and orientation were found to be 0.026 mm and 6.1 mrad through end-effector displacement and orientation ranges of 15 mm and 500 mrad respectively.

Scope and Future Work. Only CMs whose rigid equivalent

can be disaggregated into Assur groups might be modeled with the proposed technique. No consideration of buckling effects is taken into account in the deflection analysis.

Real experimental tests to validate the procedure, together with the implementation of a dynamic model, and a capable model of fully compliant mechanisms are proposals for future work.

VII. Acknowledgments

Support for this work was provided by the Colombian Administrative Department of Science, Technology and Innovation and Colombian National Service of Learning (COL-CIENCIAS – SENA) grant No. 1216-479-22001, EAFIT University (COL) and Autónoma de Manizales University (COL). The authors gratefully acknowledge this support.

References

- [1] Howell, LL. and Midha, A. A loop-closure theory for the analysis and synthesis of compliant mechanisms. *Journal of Mechanical Design*, 118:121–125, 1996.
- [2] Howell, LL. *Compliant mechanisms*. Wiley-Interscience, 2001.
- [3] Lobontiu, N. *Compliant mechanisms: design of flexure hinges*. CRC, 2003.
- [4] Venanzi, S., Giesen, P. and Parenti-Castelli, V. A novel technique for position analysis of planar compliant mechanisms. *Mechanism and Machine Theory*, 40(11):1224–1239, 2005.
- [5] Tian, Y., Shirinzadeh, B. and Zhang, D. A flexure-based five-bar mechanism for micro/nano manipulation. *Sensors and Actuators A: Physical*, 153:96–104, 2009.
- [6] Tian, Y., Shirinzadeh, B. and Zhang, D. Design and dynamics of a 3-DOF flexure-based parallel mechanism for micro/nano manipulation. *Microelectronic Engineering*, 87:230–241, 2010.
- [7] Yong, YK. and Lu, TF. Kinetostatic modeling of 3-RRR compliant micro-motion stages with flexure hinges. *Mechanism and Machine Theory*, 44(6):1156–1175, 2009.
- [8] Li, Y. and Xu, Q. Modeling and performance evaluation of a flexure-based XY parallel micro manipulator. *Mechanism and Machine Theory*, 44:2127–2152, 2009.
- [9] Saxena, A. and Kramer, SN. A simple and accurate method for determining large deflections in compliant mechanisms subjected to end forces and moments. *Journal of Mechanical Design*, 120:392–400, 1998.
- [10] Kimball, C. and Tsai, LW. Modeling of flexural beams subjected to arbitrary end loads. *Journal of Mechanical Design*, 124:223–235, 2002.
- [11] Pavlović, NT. and Pavlović, ND. Compliant mechanism design for realizing of axial link translation. *Mechanism and Machine Theory*, 44(5):1082–1091, 2009.
- [12] Pavlović, NT. and Pavlović, ND. Mobility of the compliant joints and compliant mechanisms. *Theoretical and Applied Mechanics*, 32(4):341–357, 2005.
- [13] Callegari, M., Cammarata, A., Gabrielli, A., Ruggiu, M. and Sinatra, R. Analysis and Design of a Spherical Micromechanism With Flexure Hinges. *Journal of Mechanical Design*, 131:051003.1–051003.11, 2009.
- [14] Buśkiewicz, J. A method of optimization of solving a kinematic problem with the use of structural analysis algorithm (sam). *Mechanism and Machine Theory*, 41(7):823–837, 2006.
- [15] Hansen, MR. A general method for analysis of planar mechanisms using a modular approach. *Mechanism and Machine Theory*, 31(8):1155–1166, 1996.
- [16] Zhang, Q., Zou, HJ. and Guo, WZ. Position analysis of higher-class assur groups by virtual variable searching and its application in a multifunction domestic sewing machine. *The International Journal of Advanced Manufacturing Technology*, 28(5):602–609, 2006.